A first-principles study of exchange integrals in magnetite

M Uhl† and B Siberchicot‡

† Institut für Festkörperphysik, Technische Hochschule, D-64289 Darmstadt, Germany
‡ Centre d'études de Limeil-Valenton, 94195 Villeneuve St Georges Cedex, France

Abstract. A method is presented to calculate *ab initio* exchange constants and spin-wave excitations of multi-sublattice magnetic structures on the basis of total-energy calculations of incommensurate magnetic structures. Here the exchange energies, dispersion curves and Curie temperature for magnetite (Fe_3O_4) are obtained and compared with experimental results.

1. Introduction

Ab initio calculations of exchange integrals and order temperatures for ferromagnetic 3d metals and their compounds is a non-trivial problem. Despite the success of band structure calculations in the description of ground-state properties of condensed matter, the determination of the temperature dependence of magnetic properties (and most others) meets with some difficulties. Concerning ferromagnetic metals, a number of different methods have been tried. In this context we mention the theory by Wohlfarth and Mohn [1], who determined the Curie temperatures of itinerant electron magnets from band structure calculations considering the effect of spin fluctuations via a renormalization of Landau coefficients. Another way to calculate temperature-dependent properties is by means of the disordered local moment theory (see for instance [2]).

More recently, the possibility of simulating non-collinear arrangements of spins and particularly incommensurate spin-spiral magnetic structures in elementary cells [3–7] has led to an estimate of Heisenberg exchange integrals in metals and alloys. Rather reasonable estimates of Curie temperatures were thus obtained [4–7].

In a previous paper [8] the electronic and magnetic properties of Fe_3O_4 and spinel ferrites were investigated. The aim of this work is to carry out calculations of exchange integrals for the ferrimagnetic spinel Fe_3O_4 and thus derive an estimate of its Curie temperature.

After a description of the theoretical background, calculations of exchange integrals are presented together with a calculation of the spin-wave spectrum. Finally, the results are compared and discussed in connection with other theoretical results and with experimental data.

2. Total-energy calculations of spin-spiral configurations

To make this paper reasonably self-contained we first repeat some salient theoretical points, particularly when they deviate in detail from the formulation given in earlier papers [9, 10]. The work to be described consists of self-consistent band structure and total energy calculations in the local density approximation [11, 12]. It makes use of the scalar relativistic

augmented spherical wave (ASW) method [13] suitably generalized for dealing with rather general non-collinear moment arrangements of spin-spiral configurations [9, 10]. The effective single-particle Hamilton operator $\hat{H}$ [11, 12] for spin-polarized electrons forming a non-collinear magnetic order is as usual obtained from the Euler–Lagrange equations minimizing the total energy as a functional of the density matrix, and may be written in bi-spinor form as [14, 15]

$$\hat{H} = -\nabla^2 1 + \sum_{j\nu} \mathbf{U}_{j\nu}^+ \mathbf{V}_\nu (r - t_{j\nu}) \mathbf{U}_{j\nu}. \tag{2.1}$$

Here we use the label j to designate the unit cell and the label ν the basis atom, and we imply an atomic-sphere approximation, i.e. the effective potential $\mathbf{V}_\nu$ is defined to vanish outside its respective atomic-sphere radius. The quantity $\mathbf{U}_{j\nu}$ is the standard spin-$\frac{1}{2}$-rotation matrix

$$\mathbf{U}_{j\nu} = \begin{pmatrix} \cos(\theta_\nu/2) & \sin(\theta_\nu/2) \\ -\sin(\theta_\nu/2) & \cos(\theta_\nu/2) \end{pmatrix} \begin{pmatrix} \exp(+\mathrm{i}q \cdot t_{j\nu}/2) & 0 \\ 0 & \exp(-\mathrm{i}q \cdot t_{j\nu}/2) \end{pmatrix} \tag{2.2}$$

which describes a transformation between a global and a local spin coordinate system where the directions of the local magnetization at the sites designated by the translation vectors $\{t_{j\nu}\}$ are given by the polar angles $\{\theta_{j\nu}, \phi_{j\nu}\}$ defining a spin-spiral configuration of a spin-wave vector q: $\theta_{j\nu} = \theta_\nu$ and $\phi_{j\nu} = q \cdot t_{j\nu}$.

In this case the Hamiltonian given by (2.1) commutes with generalized translations defined by Herring [16], who showed that a generalized Bloch theorem can be used to construct the eigenfunctions of the problem defined by (2.1) [14–16]. This means in particular that for any choice of the wave vector q it is the chemical Brillouin zone that constitutes the domain for the k-vectors to be used for sampling the elements of the density matrix. This makes self-consistent calculations feasible even for cases with a non-trivial unit cell, like that of Fe_3O_4. For a detailed description of calculating incommensurate spin spiral configurations with the non-collinear ASW method see [9, 10].

3. Calculation of exchange constants

To calculate spin-wave excitations of Fe_3O_4 we assume the magnetic moments to be localized. By this we mean that we can describe the spin system by the Heisenberg Hamiltonian

$$\hat{H} = -\sum_{i\mu, j\nu} J_{\mu\nu}(t_{i\mu} - t_{j\nu})\hat{S}(t_{i\mu}) \cdot \hat{S}(t_{j\nu}). \tag{3.1}$$

Here $\hat{S}(t_{j\nu})$ is the spin located at the magnetic site labelled by $t_{j\nu}$ and $J_{\mu\nu}(t_{i\mu} - t_{j\nu})$ is the exchange constant that describes the interaction between the spins at the sites $t_{i\mu}$ and $t_{j\nu}$. Treating the spins as classical observables in a spin-spiral configuration, we may prescribe the direction of a spin $S(t_{j\nu})$ by its length S_ν, its polar angle θ_ν, and the spiral vector q expressed in cartesian coordinates as

$$S(t_{j\nu}) = S_\nu \big(\cos(q \cdot t_{j\nu}) \sin\theta_\nu, \sin(q \cdot t_{j\nu}) \sin\theta_\nu, \cos\theta_\nu \big). \tag{3.2}$$

Thus in a spin-spiral configuration the magnetic exchange energy per unit cell is given by:

$$E(q, \{\theta_v\}) = \frac{1}{N} \sum_{i\mu, j\nu} S_\mu S_\nu J_{\mu\nu}(t_{i\mu} - t_{j\nu})\big(\cos(q \cdot (t_{i\mu} - t_{j\nu}))\sin\theta_\mu \sin\theta_\nu + \cos\theta_\mu \cos\theta_\nu\big).$$

$$(3.3)$$

The crystal structure of Fe_3O_4 is shown in figure 1. Here the iron ions are located at two antiparallel ordered sublattices A and B, consisting of two tetrahedral Fe_A sites ($A1$, $A2$) and four octahedral Fe_B-sites ($B1-B4$). Here the classical ferrimagnetic ground state can be treated as a two-sublattice collinear Néel configuration [17]. In our calculations we pivot the spins of the iron sites only, see figure 2. Thus (3.3) gives

$$
\begin{aligned}
E(q, \theta_A, \theta_B) = &-S_A^2 \sum_{\alpha \in AA} n_{AA}(R_\alpha) J_{AA}(R_\alpha)[\cos(q \cdot R_\alpha)\sin^2\theta_A + \cos^2\theta_A] \\
&- S_B^2 \sum_{\beta \in BB} n_{BB}(R_\beta) J_{BB}(R_\beta)[\cos(q \cdot R_\beta)\sin^2\theta_B + \cos^2\theta_B] \\
&+ S_A S_B \sum_{\gamma \in AB} n_{AB}(R_\gamma) J_{AB}(R_\gamma)[\cos(q \cdot R_\gamma)\sin\theta_A \sin\theta_B + \cos\theta_A \cos\theta_B] \\
&+ \cos\theta_A n_A I_{AC} + \cos\theta_B n_B I_{BC}
\end{aligned}
$$

$$(3.4)$$

where the size of the spin S_A and the angle θ_A refer to the tetrahedral Fe^A site, and S_B, θ_B refer to the octahedral Fe^B site. Furthermore J_{AA}, J_{BB} and J_{AB} are appropriate exchange constants between the iron atoms and n_{AA}, n_{BB} and n_{AB} their weights per unit cell. Finally, I_{AC} and I_{BC} describe the exchange energy between an iron site and the 'background', caused by a small magnetization of the oxygen and empty sphere sites.
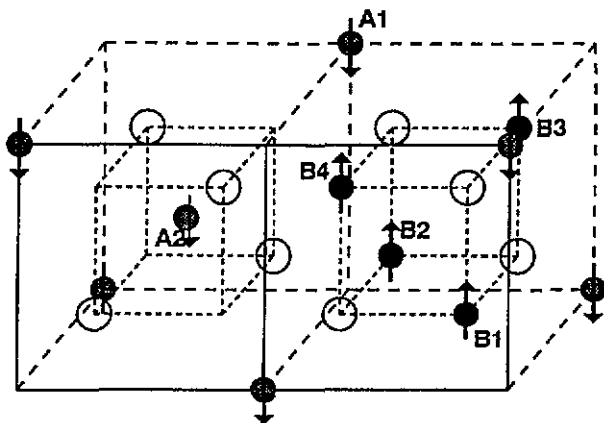

Figure 1. Two octants of the spinel structure of magnetite. The spins and the positions of the iron sites are labeled. The open circles represent oxygen sites. (From Glasser and Milford [18]).

Using (3.4) the exchange constants $J_{AA}(R_\alpha)$, $J_{BB}(R_\beta)$ and $J_{AB}(R_\gamma)$ can easily be calculated by

$$S_A^2 n_{AA}(R_\alpha) J_{AA}(R_\alpha) = \frac{-1}{N\sin^2\theta} \int d^3q \cos(q \cdot R_\alpha)\big(E(q, \theta, 0) - E(0, \theta, 0)\big)$$

$$S_B^2 n_{BB}(R_\beta) J_{BB}(R_\beta) = \frac{-1}{N\sin^2\theta} \int d^3q \cos(q \cdot R_\beta)\big(E(q, 0, \theta) - E(0, 0, \theta)\big)$$

$$(3.5)$$

$$
\begin{aligned}
S_A S_B n_{AB}(R_\gamma) J_{AB}(R_\gamma) = &\frac{-1}{N\sin^2\theta} \int d^3q \cos(q \cdot R_\gamma)\big(E(q, \theta, \theta) - E(0, \theta, \theta)\big) \\
&- S_A^2 n_{AA}(R_\gamma) J_{AA}(R_\gamma) - S_B^2 n_{BB}(R_\gamma) J_{BB}(R_\gamma)
\end{aligned}
$$

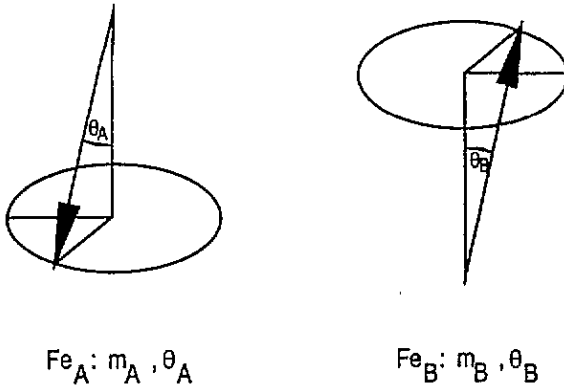$$Fe_A: m_A, \theta_A \qquad\qquad Fe_B: m_B, \theta_B$$

Figure 2. Orientation of excited spins of the Fe^A sites and the Fe^B sites; compare also figure 1.

where the quantities $E(q, \theta_A, \theta_B)$ are obtained by total-energy calculations. Since the ground state of magnetite is ferrimagnetic we get $E(q, \theta_A, \theta_B) > E(0, 0, 0)$ for all states.

4. Calculation of the spin-wave spectrum

To calculate spin-wave energies we make the spin-wave approximation of considering the z components to be invariant and keeping only terms linear in the transverse components. Thus we rewrite the Hamiltonian of (3.1) as follows:

$$\hat{H} = - \sum_{i\mu, j\nu} J_{\mu\nu}(t_{i\mu} - t_{j\nu})\big(\hat{S}^z(t_{i\mu})\hat{S}^z(t_{j\nu}) + \hat{S}^+(t_{i\mu})\hat{S}^-(t_{j\nu})\big). \qquad (4.1)$$

In Fe_3O_4 the ground state can be approximated by a collinear ferrimagnetic eigenstate of two antiparallel ordered sublattices $\{A\}$ and $\{B\}$ (Néel [17]), which may be specified as $|0\rangle = \prod_{j\nu} |\lambda_\nu S_\nu(t_{j\nu})\rangle$. Here $S_\nu(t_{j\nu})$ denotes the spin located at the site $t_{j\nu}$ and λ_ν the direction of its magnetization, i.e. $\lambda_\nu = -1$ for a tetrahedral site ($\nu \in A$) and $\lambda_\nu = +1$ for an octahedral site ($\nu \in B$). The corresponding energy of the Néel ground state is

$$\epsilon_0 = - \sum_{i\mu, j\nu} J_{\mu\nu}(t_{i\mu} - t_{j\nu})\lambda_\mu\lambda_\nu S_\mu(t_{i\mu})S_\nu(t_{j\nu}).$$

Using Bloch's theorem the spin-wave energies $\epsilon(k)$ are determined by

$$\hat{H}|k\rangle = \big(\epsilon_0 + \epsilon(k)\big)|k\rangle \qquad (4.2)$$

and

$$|k\rangle = \frac{1}{\sqrt{2N}} \sum_\nu C_\nu(k) \sum_j \exp(ik \cdot t_{j\nu})\hat{S}^-(t_{j\nu})|0\rangle. \qquad (4.3)$$

Analogous to Glasser and Milford [18] and Nauciel and co-workers [19], but now including not only nearest-neighbour interactions, the solution of the eigenvalue problem defined by (4.2) and (4.3) leads to the following secular equation:

$$\sum_\mu \lambda_\mu S_\mu E_{\mu\nu}(0)C_\nu(k) - \sum_\mu \lambda_\nu S_\nu E_{\nu\mu}(k)C_\mu(k) = \epsilon(k)C_\nu(k) \qquad (4.4)$$

where $E_{\nu\mu}(k)$ are calculated by Fourier transformation of the exchange constants between the sites ν and μ:

$$E_{\nu\mu}(k) = 2 \sum_j \exp[ik \cdot (t_{j\nu} - t_{0\mu})]J_{\mu\nu}(t_{j\nu} - t_{0\mu}). \qquad (4.5)$$

5. Results and discussion

Since the touching muffin-tin spheres only fill about 40% of the volume of the unit cell, we choose a set of 18 additional so-called 'empty spheres' (ES) [8]. Thus, in the space group Fd3m [20, 21], the calculations are done with 32 sites per unit-cell, i.e. two iron sites Fe^A at the Wyckoff positions (a), four iron sites Fe^B at (d), eight oxygen sites O at (e), two ES at (b), four ES at (c) and, finally, twelve ES at (f). The lattice constant is given by $a = 8.394\,\text{Å}$ [8, 22] and for the Wigner–Seitz radii we use the values of Pénicaud and co-workers [8].

To calculate the density of states self-consistently we employ a set of 216 k points spread uniformly over the full Brillouin zone. Whereas the collinear ferrimagnetic ground state has the full cubic symmetry (O_h), in excited spin-spiral configurations the symmetry is reduced and given by group elements $\{D\}$, which keep the spiral vector q invariant: $Dq = q$ [15, 23]. Therefore, the number of irreducible k points varies from 28 in the case of the ferrimagnetic ground state to 216 in the case of spin-spiral configurations that possess no symmetry.

To describe spin waves by fixed spin-spiral calculations, we pivot the angles of the magnetic Fe^A and Fe^B sites, see figure 2. To include all magnetic exchange contributions, i.e. Fe^A–Fe^A, Fe^B–Fe^B and Fe^A–Fe^B interactions, we do spin-spiral calculations with (i) $\theta_A = 30°$ and $\theta_B = 30°$. Furthermore, to obtain the Fe^A–Fe^A and Fe^B–Fe^B contributions separately, we use (ii) $\theta_A = 30°$ and $\theta_B = 0°$ and (iii) $\theta_A = 0°$ and $\theta_B = 30°$. To obtain reasonable values of exchange constants by comparing total energies of the three series for the same values of q, we assume here that the magnetic moments of the Fe^A and Fe^B sites are well localized, i.e. the change in the magnetic moment $\Delta m_{Fe} < 0.05\mu_B$ with different magnetic configurations. Since the magnetic moments of the oxygen- and empty-sphere sites m_O, m_{ES}, are small ($< 0.2\mu_B$), we do not pivot the spin directions of these sites and neglect their magnetic contributions.

To calculate all exchange constants $J(x)$ with $x = (x_1, x_2, x_3)$ up to $|x_1|, |x_2|, |x_3| \leqslant a$ by Fourier summation of the exchange energies $E(q)$, one has to choose a cubic mesh of spiral vectors q with $\Delta q_1 = \Delta q_2 = \Delta q_3 = \pi/a$. Since the reciprocal volume of the Brillouin zone Ω_0 is $|\Omega_0| = 4(2\pi/a)^3$, we require 32 q points per Brillouin zone.

Since all magnetic sites of magnetite are fixed on positions of a Jones lattice given by a body centred cubic structure with a lattice constant of $a' = \frac{1}{4}a$, see figure 1, the exchange energy $E(q, \{\theta_\nu\})$ (and in particular $E(q, 30°, 30°)$) is periodic with the Jones zone Ω_{AB} having a volume of $|\Omega_{AB}| = 128(2\pi/a)^3 = 32|\Omega_0|$. In other words the total energy of (3.4), $E(q, \theta_A, \theta_B)$, describes 32 modes in the Brillouin zone.

In the same manner, to calculate the *single-sublattice excitations* $E(q, 30°, 0°)$ by a pivot of only Fe^A spins and $E(q, 0°, 30°)$ by a pivot of only Fe^B spins, one can restrict the reciprocal space to the Jones zone Ω_{AA} (Ω_{BB}) defined by the Fe^A sites (Fe^B sites), i.e. $|\Omega_{AA}| = 4|\Omega_0|$ and $|\Omega_{BB}| = 8|\Omega_0|$.

Thus, the exchange constants $J_{AB}(x)$ ($J_{AA}(x)$, $J_{BB}(x)$) are calculated by (3.5) using a mesh of 1024 (128, 256) q points in Ω_{AB} (Ω_{AA}, Ω_{BB}).

Figure 3 shows the calculated energy contributions of (3.5): (a) $E_{AA}(q) = E(q, 30°, 0°) - E(0, 30°, 0°)$, (b) $E_{BB}(q) = E(q, 0°, 30°) - E(0, 0°, 30°)$, and (c) $E_{AB}(q) = E(q, 30°, 30°) - E(0, 30°, 30°)$, fitted by (3.4). Since the spin excitations are obtained by ground-state calculations of spin-spiral configurations, we multiply total energies by the *ad hoc* factor $S/(S+1)$ for (3.5). Here we use $S_A = \frac{5}{2}$ and $S_B = \frac{9}{4}$, which gives a total magnetization of $S = 4S_B - 2S_A = 4$ [18, 19, 24].

In table 1 we list the exchange constants $J_{AA}(x)$, $J_{BB}(x)$ and $J_{AB}(x)$, see (3.5). The quantities $n_{AA}(x)$, $n_{BB}(x)$ and $n_{AB}(x)$ of table 1 denote the number of times they appear

(a)

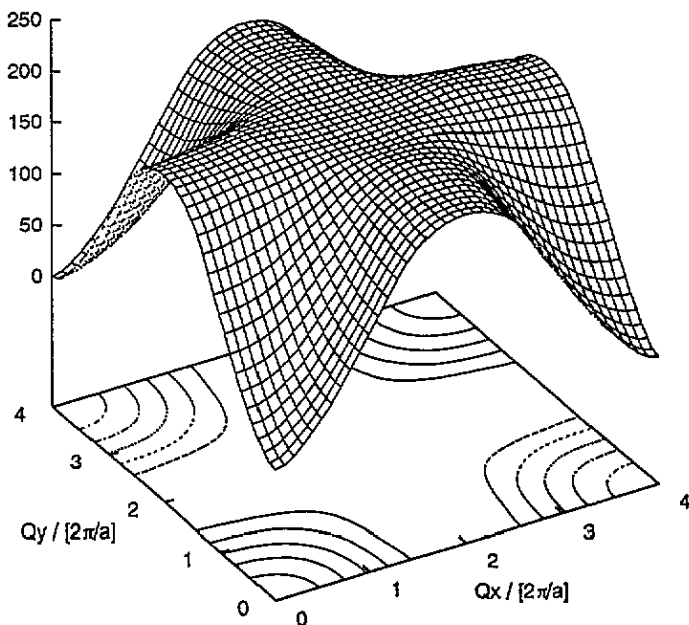$E_{AA}(q)$ / [meV/u.c.]
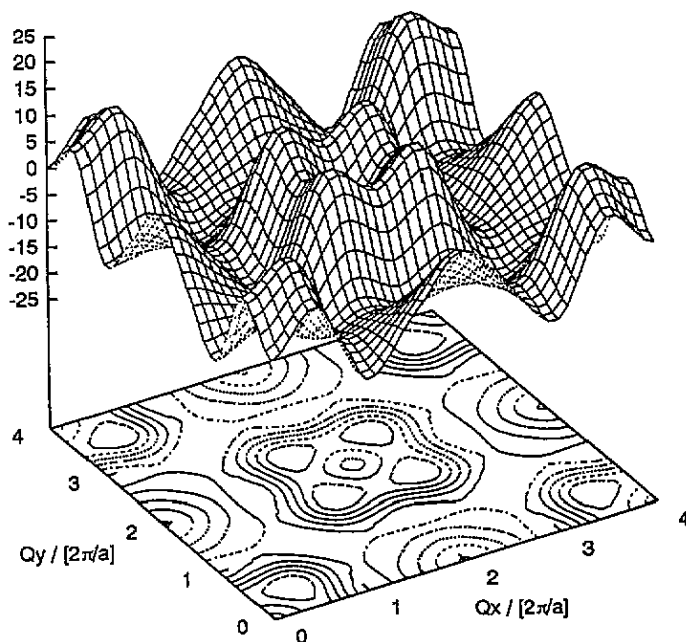
(b)

$E_{BB}(q)$ / [meV/u.c.]

Figure 3. Calculated energy differences of spin-spiral configurations. (a) Single-Fe^A-sublattice excitations: $\theta_A = 30°$, $\theta_B = 0°$. (b) Single-Fe^B-sublattice excitations: $\theta_A = 0°$, $\theta_B = 30°$. (c) Excitations including both sublattices: $\theta_A = 30°$, $\theta_B = 30°$.

(c)

$E_{AB}(q)$ / [meV/u.c.]
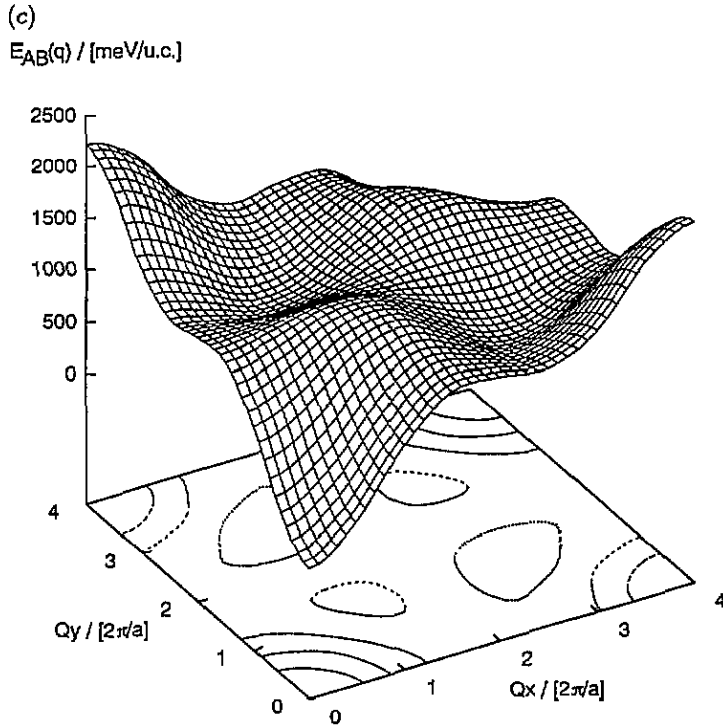

Figure 3. (Continued)

in the unit cell. Furthermore, the total exchange energies of the sublattices $\tilde{J}_{AA}$, $\tilde{J}_{BB}$ and $\tilde{J}_{AB}$ are also calculated.

Table 2 shows a comparison of calculated and experimental values of nearest-neighbour exchange constants. Our results confirm that the nearest-neighbour exchange constant between the Fe^A and the Fe^B sublattices, $J_{AB}^{NN} = J_{AB}(1,1,3)$, plays a dominant role [18, 25–28]. Since J_{AB}^{NN} is negative, the sublattices order antiparallel. Moreover, the magnetic exchange between neighbouring A sites $J_{AA}^{NN} = J_{AA}(2,2,2)$ and neighbouring B sites $J_{BB}^{NN} = J_{BB}(0,2,2)$ give substantial contributions to the exchange energy.

In agreement with experimental values we obtain ferromagnetic coupling between neighbouring B sites ($J_{BB}^{NN} > 0$) and antiferromagnetic coupling between neighbouring A sites ($J_{AA}^{NN} < 0$) [17, 18, 24, 28–31]. From figure 3(a) it is seen that the energy difference $E_{AA}(q)$ is negative over a wide portion of the Brillouin zone, whereas $E_{BB}(q)$ (figure 3(b)) and $E_{AB}(q)$ (figure 3(c)) give positive contributions for all values of q.

In the second line of table 2 the constants J_{AA}^{NN}, J_{BB}^{NN} and J_{AB}^{NN} are determined in the nearest-neighbour approximation; i.e. they are calculated by setting all other constants to zero ($J(x) = 0$ for $|x| \geqslant 0.5a$). Furthermore table 1 shows that for distances $|x| \geqslant 0.9a$ the exchange constants become very small and can be neglected.

In figure 4 the calculated spin-wave dispersion curves are shown along lines of high symmetry, Δ, Σ and Λ. Here the notation ($\omega_1, \ldots, \omega_6$) is that given in [18, 19]. Within the nearest-neighbour approximation their values at the Γ point are given by [18]

$$\hbar\omega_3 = 0 \qquad \hbar\omega_4 = 24 J_{AB}^{NN} S_B - 12 J_{AB}^{NN} S_A \qquad \hbar\omega_1 = \hbar\omega_5 = \hbar\omega_6 = 12 J_{AB}^{NN} S_A - 16 J_{BB}^{NN} S_B$$

$$\hbar\omega_2 = 24 J_{AB}^{NN} S_B - 16 J_{AA}^{NN} S_A.$$

Table 1. Magnetic exchange constants $J_{AA}(x)$, $J_{BB}(x)$ and $J_{AB}(x)$, calculated by (3.5), and total exchange energies $\bar{J}_{AA}$, $\bar{J}_{BB}$ and $\bar{J}_{AB}$. $\bar{J}_{AA} = \sum_x n_{AA}(x)J_{AA}(x) = -1.1$ mev, $\bar{J}_{BB} = \sum_x n_{BB}(x)J_{BB}(x) = 19.9$ mev and $\bar{J}_{AB} = \sum_x n_{AB}(x)J_{AB}(x) = -135.4$ mev.

x [a/8]	$|x|$ [a]	$n_{AA}(x)$	$J_{AA}(x)$ [meV]	$n_{BB}(x)$	$J_{BB}(x)$ [meV]	$n_{AB}(x)$	$J_{AB}(x)$ [meV]
(0,2,2)	0.354			24	0.831		
(1,1,3)	0.415					48	−2.877
(2,2,2)	0.433	8	−0.179				
(2,2,4)	0.612			48	−0.015		
(3,3,3)	0.650					16	0.056
(1,1,5)	0.650					48	0.025
(0,4,4)	0.707	24	−0.063	48	0.015		
(0,2,6)	0.791			48	−0.041		
(3,3,5)	0.820					48	0.049
(2,2,6)	0.829	24	0.058				
(2,4,6)	0.935			96	0.011		
(3,5,5)	0.960					48	−0.022
(1,3,7)	0.960					96	0.017
(0,0,8)	1.000	12	0.032	24	0.008		
(0,6,6)	1.061			24	0.018		
(2,2,8)	1.061			48	0.011		
(5,5,5)	1.083					16	−0.004
(1,5,7)	1.083					96	−0.002
(2,6,6)	1.090	24	0.010				
(4,6,6)	1.173			48	−0.004		
(4,4,8)	1.225	48	−0.003	96	−0.002		
(2,6,8)	1.275			96	−0.000		
(3,7,7)	1.293					48	0.003
(6,6,6)	1.299	8	0.010				
(5,7,7)	1.386					48	0.006
(0,8,8)	1.414	24	0.004	48	−0.004		
(6,6,8)	1.458			48	0.003		
(8,8,8)	1.732	16	0.000	32	0.001		

Table 2. Calculated and experimental values of nearest-neighbour exchange constants in Fe_3O_4.

	J_{AA}^{NN} [meV]	J_{BB}^{NN} [meV]	J_{AB}^{NN} [meV]
This calculation	−0.18	+0.83	−2.88
This calculation, NN app.	−0.11	+0.63	−2.92
Néel [17]	−1.50	+0.04	−2.00
Glasser and Milford [18]	0	+0.24	−2.40
Gr. Diff. In. Neutrons [29]	−1.56	+0.26	−2.38
Möglestue [30]	−1.52	+0.31	−2.42

Contrary to some experiments we obtain $\hbar\omega_1 < \hbar\omega_2$ at the Γ point, or equivalently $(3J_{AB}^{NN} + 4J_{AA}^{NN})S_A < (6J_{AB}^{NN} + 4J_{BB}^{NN})S_B$, because our value J_{AA}^{NN} is much smaller than the values of J_{AB}^{NN} and also J_{BB}^{NN}, but is not of comparable magnitude to J_{AB}^{NN} as in [17, 28–30]. Therefore we cannot verify a crossing of the ω_1 and ω_2 branches along the symmetry line Δ and our dispersion curves differ from those of [17, 28] in particular with respect to the ω_2 branch, but it is in good agreement with the approximation of Glasser and Milford [18], where $J_{AA}^{NN} = 0$ and $J_{BB}^{NN} = -0.1 J_{AB}^{NN}$.

Since the magnitude of exchange constants $J(x)$ decreases quickly with increasing values of $|x|$, the branches ω_5 and ω_6 are nearly constant over the whole Brillouin zone, in agreement with the nearest-neighbour approximation.
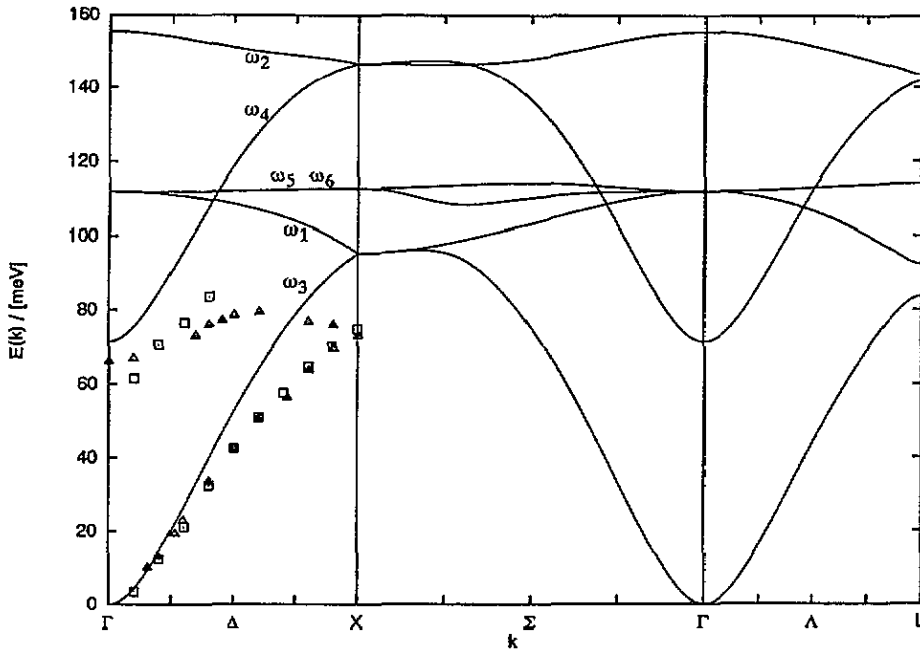
Figure 4. Calculated acoustic and optic spin-wave dispersion curve of magnetite for k vectors along the symmetry lines Δ, Σ and Λ in the Brillouin zone. The squares show the data of Watanabe and Brockhouse [25] and the triangles are experimental results of [29].

In comparison to experiments our values of exchange energies are about 20% too large. We assume that this is caused by constraining the directions of spins. Expensive self-consistent calculations of angles at all sites would slightly reduce the spin-spiral energies and exchange constants.

Since the experimental two-sublattice exchange constants are not in good agreement with the predictions of superexchange theory, Srivastava and co-workers [31] investigated a three-sublattice model where the spins on the two Fe^B sites are localized with $S_{B'} = 2.0$ and $S_{B''} = 2.5$. In our calculations a change of the spins would yield slight differences in the spectrum, but it does not play a dominant role like the magnitude or the ratio of the exchange constants.

The magnitude of the spin-wave stiffness constant describes the second derivative of the acoustic branch ω_3 at $k = 0$ [24, 32]:

$$\epsilon(k) = Dk^2 = \left(\sum_{ij} (k \cdot t_{ij})^2 \lambda_i \lambda_j S_i S_j J_{ij}(t_{ij}) \right) \left(\sum_i \lambda_i S_i \right)^{-1}. \tag{5.1}$$

For magnetite in the nearest-neighbour approximation, (5.1) leads to [24]:

$$D^{NN} = a^2 \frac{2J_{AA}^{NN} S_A^2 + 4J_{AB}^{NN} S_B^2 - 11J_{AB}^{NN} S_A S_B}{32S_B - 16S_A}. \tag{5.2}$$

Our calculations give $D = 715 \, \text{meV} \, \text{Å}^2$, if we take into account all exchange constants (5.1), and $D^{NN} = 423 \, \text{meV} \, \text{Å}^2$ in the nearest-neighbour approximation (5.2). The latter

value is in good agreement with other nearest-neighbour approximations of Brockhouse and Watanabe [33] (443 meV Å^2) and Srivastava and Aiyar [24] (318 meV Å^2). This result shows that the nearest-neighbour approximation for the determination of the stiffness constant has to be used with caution.

To estimate the Curie temperature within the mean-field approximation, the magnetization near T_C is determined by the following secular equation:

$$\frac{2S_\nu(S_\nu+1)}{3}\sum_{i\mu}J_{\mu\nu}(t_{0\nu}-t_{i\mu})M_\mu(T)=k_BT_CM_\nu(T) \tag{5.3}$$

see for example [34, 35]. In the two-sublattice model of magnetite the solution of (5.3) is given by

$$k_BT_C=a\tilde{J}_{AA}+b\tilde{J}_{BB}+[(a\tilde{J}_{AA}-b\tilde{J}_{BB})^2+ab\tilde{J}_{AB}^2]^{1/2} \tag{5.4}$$

where

$$a=\frac{S_A(S_A+1)}{3n_A} \qquad b=\frac{S_B(S_B+1)}{3n_B}.$$

Here our computed values of the exchange constants give $k_BT_C=139$ meV ($T_C=1612$ K) which is too high compared with the experimental value of $T_C=858$ K, see also the discussion and table 1 of Glasser and Milford [18].

Finally, considering recent publications [24, 27, 28] we find that the situation of magnetite is quite controversial. At 122 K a Vervey phase transition is observed [36, 37]. Above the transition temperature magnetite possesses a high conductivity, whereas below there exists an insulating state, being presumably brought about by a band splitting. Our calculations describe, as do previous calculations [8, 22, 38], the metallic high-temperature phase and not the insulating ground state, which poses an open problem [8].

In this work it has been our purpose to investigate the magnetic properties of the high-temperature phase and to calculate magnetic exchange constants, spin excitations and the Curie temperature within the Heisenberg model. Using incommensurate non-collinear spin-spiral configurations we get reasonable results for the exchange constants and spin-wave energies, even though all values are a little too large, in particular the Curie temperature. Because of these discrepancies this can only be a first step, but still it shows that the method shown here allows us to examine the magnetic properties of complex structures with localized moments.

References

[1]   Wohlfarth E P and Mohn P 1988 *Physica* B+C **149** 145
[2]   Gyorffy B L, Pindor A J, Staunton J, Stocks G M and Winter H 1985 *J. Phys. F: Met. Phys.* **15** 1337
[3]   You M V and Heine V 1982 *J. Phys. F: Met. Phys.* **12** 177
[4]   Luchini M U and Heine V 1989 *J. Phys.: Condens. Matter* **1** 8961
[5]   Sandratskii L M and Guletskii P G 1989 *J. Magn. Magn. Mater.* **79** 306

[6] Liechtenstein A I, Katsnelson M I, Antropov V P and Gubanov V A 1987 *J. Magn. Magn. Mater.* **67** 65
[7] Uhl M 1991 *Diplomarbeit* (TH Darmstadt) unpublished
[8] Pénicaud M, Siberchicot B, Sommers C B and Kübler J 1992 *J. Magn. Magn. Mater.* **103** 212
[9] Uhl M, Sandratskii L M and Kübler J 1992 *J. Magn. Magn. Mater.* **103** 314
[10] Uhl M, Sandratskii L M and Kübler J 1994 *Phys. Rev.* B **50** 291
[11] Kohn W and Sham L J 1965 *Phys. Rev.* A **140** 1133
[12] von Barth U and Hedin L 1972 *J. Phys. C: Solid State Phys.* **5** 1629
[13] Williams A R, Kübler J and Gelatt C D Jr 1979 *Phys. Rev.* B **19** 6094
[14] Sandratskii L M 1986 *Phys. Status Solidi* b **135** 167
[15] Sandratskii L M 1990 *Solid State Commun.* **75** 527
[16] Herring C 1966 *Magnetism IV* ed G Rado and H Suhl (New York: Academic) ch V, XIII
[17] Néel L 1948 *Ann. Phys.* **3** 137
[18] Glasser M L and Milford F J 1963 *Phys. Rev.* **130** 1783
[19] Nauciel-Bloch M, Hennion B and Sarma G 1970 *Solid State Commun.* **8** 2141
[20] Kaplan T A 1958 *Phys. Rev.* **109** 782
[21] *Int. Tables of X-ray Crystallography*
[22] Yanase A and Siratori K 1984 *J. Phys. Soc. Japan* **53** 312
[23] Sandratskii L M 1991 *J. Phys.: Condens. Matter* **3** 8565, 8587
[24] Srivastava C M and Aiyar R 1987 *J. Phys. C: Solid State Phys.* **20** 1119
[25] Watanabe H and Brockhouse B N 1962 *Phys. Lett.* **1** 189
[26] Torrie B H 1967 *Solid State Commun.* **5** 715
[27] Aragón R 1992 *Phys. Rev.* B **46** 5328
[28] De Grave E, Persoons R M, Vandenberghe R E and de Bakker P M A 1993 *Phys. Rev.* B **47** 5881
[29] Groupe de Diffusion Inélastique des Neutrons 1971 *J. Phys.* C **1** 1182
[30] Möglestue K T 1968 *IAEA Congress of Copenhagen* **2** 117
[31] Srivastava C M, Srinivasan G and Nanandikar N G 1979 *Phys. Rev.* B **19** 499
[32] Keffer F 1966 *Handbuch der Physik 28, part 2* ed H P J Wijn (Berlin: Springer) p 1
[33] Brockhouse B N and Watanabe H 1961 *IAEA Congress of Vienna* **11** 297
[34] Nolting W 1986 *Quantentheorie des Magnetismus* (Stuttgart: Teubner)
[35] Rado G T and Folen V J 1960 *J. Appl. Phys.* **31** 62
[36] Verwey E J W and Haayman P W 1941 *Physica* **8** 979
[37] Iida S, Mizushima K, Mizoguchi H, Mada J, Umemura S, Nakoo K and Yoshida J 1976 *Magnetism and Magnetic Materials (1975)* ed J J Becker, G H Lander and J J Rhyne (New York: AIP)
[38] de Groot R A and Buschow K H J 1986 *J. Magn. Magn. Mater.* **54–7** 1377